2009

Effect of large strain on dielectric and ferroelectric properties of Ba0.5Sr0.5TiO3 thin films

Bo Xiao
Virginia Commonwealth University, xiaob@vcu.edu

Vitaliy Avrutin
Virginia Commonwealth University, vavrutin@vcu.edu

Hongrui Liu
Virginia Commonwealth University

See next page for additional authors

Xiao, B., Avrutin, V., Liu, H., et al. Effect of large strain on dielectric and ferroelectric properties of Ba0.5Sr0.5TiO3 thin films. Applied Physics Letters, 95, 012907 (2009).

Effect of large strain on dielectric and ferroelectric properties of $Ba_{0.5}Sr_{0.5}TiO_3$ thin films

Bo Xiao,[1,a)] Vitaliy Avrutin,[1] Hongrui Liu,[1] Emmanuel Rowe,[1] Jacob Leach,[1] Xing Gu,[1] Ümit Özgür,[1] Hadis Morkoç,[1] W. Chang,[2] L. M. B. Alldredge,[2] S. W. Kirchoefer,[2] and J. M. Pond[2]

[1]*Department of Electrical and Computer Engineering, Virginia Commonwealth University, Richmond, Virginia 23284, USA*

[2]*Naval Research Laboratory Washington, Washington, DC 20375, USA*

(Received 14 May 2009; accepted 18 May 2009; published online 8 July 2009)

$Ba_xSr_{1-x}TiO_3$ is ideally suited as a tunable medium for radio frequency passive component. In this context we have studied the effect of biaxial strain on the dielectric and ferroelectric properties of $Ba_{0.5}Sr_{0.5}TiO_3$ thin films grown epitaxially on $SrTiO_3$ (001) substrates. The lattice parameters of the films determined by high-resolution x-ray diffraction with the thickness varying from 160 to 1000 nm indicated large biaxial compressive strain which decreased from 2.54% to 1.14% with increasing film thickness. Temperature-dependent measurements of the dielectric constant in our strained $Ba_{0.5}Sr_{0.5}TiO_3$ thin films revealed a significant increase in the Curie temperature as the film thickness is below 500 nm. Enhanced ferroelectric behavior was observed for highly strained films with a remanent polarization of 15 $\mu C/cm^2$ in the 160-nm-thick layer. However, the thick films ($\geq$500 nm) exhibited weak temperature dependence of the dielectric constant without any pronounced peak corresponding to the Curie temperature, which may suggest inhomogeneous strain distribution in the thick films. © *2009 American Institute of Physics*. [DOI: 10.1063/1.3151961]

Ferroelectric materials have been extensively studied and become important for a variety of applications such as nonvolatile random access memory devices, nonlinear optics, motion and thermal sensors, and tunable microwave devices. $Ba_xSr_{1-x}TiO_3$ (BST) as one of widely studied ferroelectric materials is of paramount interest as medium for tunable microwave passive components.[1,2] Most of studies are focused on BST thin films because of the low cost and possible integration with mature semiconductor technologies, which differ drastically from the corresponding bulk material due to the presence of strain in the thin films. Strain in BST thin films is found to be a significant factor affecting the Curie temperature and dielectric properties.[3,4] Therefore, tailoring strain provides an alternative approach to changing the barium-to-strontium ratio. Strain has already been utilized in mainstream semiconductor industry to enhance device performance.[5] This approach generally referred as strain engineering has been extended to alter certain properties of ferroelectric materials. For example, notable change in the Curie temperature and enhancement of ferroelectric properties were noted in strained strontium titanate ($SrTiO_3$) (Ref. 6) and barium titanate ($BaTiO_3$) (Ref. 7) thin films. Strained films exhibited improved ferroelectric and dielectric properties compared to the intrinsic properties of the unstrained bulk materials. As a perovskite material, strontium titanate, $SrTiO_3$ (STO) has been widely used as the substrate for oxide heteroepitaxy. The similar crystal structure and close thermal expansion coefficient between BST and STO make STO a convenient substrate for growing high quality BST thin films. In this study, we have investigated strain-induced structural properties and dielectric constant as a function of temperature for a series of $Ba_{0.5}Sr_{0.5}TiO_3$ thin films grown on $SrTiO_3$ substrates with different thickness.

BST thin films were grown epitaxially by off-axis rf magnetron sputtering using a 3-inch-diamater $Ba_{0.5}Sr_{0.5}TiO_3$ stoichiometric target. Ar and O_2 gases were introduced into the growth chamber through mass flow controllers to maintain the growth chamber pressure at 2 mTorr with an Ar-to-O_2 ratio of 6:1. During growth, the substrate temperature was nominally 750 °C according to the thermocouple reading, and the rf sputtering power was set at 120 W. These growth conditions yielded a deposition rate of about 450 Å/h for the $Ba_{0.5}Sr_{0.5}TiO_3$ (BST) layers.

The crystal structure and lattice parameters of the as-deposited BST films were determined by high resolution x-ray diffraction (HRXRD). High structural perfection of the BST thin films has been revealed by HRXRD 2θ-ω and ω-rocking curve scans. All BST thin films exhibited exclusively (00l) reflections and narrow ω-rocking curves. The full width at half-maximum (FWHM) of the (001) rocking curves is about 2.4 arc min for the films with a thickness of 500 nm or less. For 1000-nm-thick BST films, the generation of misfit and threading dislocations caused an increase in the FWHM value of the (001) rocking curve to 3.6 arc min. The lattice parameters of the BST thin films were calculated from the symmetric (001) and asymmetric (011) XRD patterns. The peak positions of HRXRD reflections from the BST films were calibrated using reflections from the STO substrate as reference. Figure 1 shows the symmetric and asymmetric HRXRD scans of 160-, 300-, and 1000-nm-thick BST films, which clearly indicate a shift of the BST peak as the thickness changes. Both (001) and (011) reflections from the BST thin films are shifted to lower angles as compared to $2\theta_{(001)}=22.494°$ and $2\theta_{(011)}=32.032°$ for bulk BST of the same composition.[8] As the thickness increases, one notes that the BST peak positions approach the bulk values.

The out-of-plane lattice parameter c for the BST films investigated was calculated directly from the (001) reflec-

a)Electronic mail: xiaob@vcu.edu.

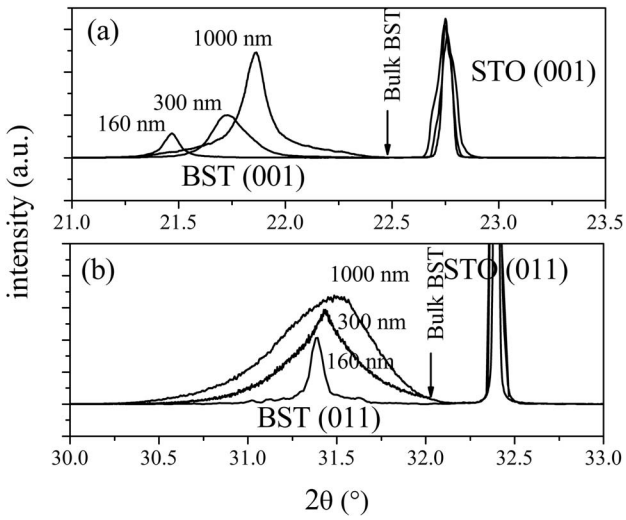

FIG. 1. XRD patterns of BST thin films with the thickness ranging from 160 to 1000 nm: (a) symmetric (001) 2θ-ω scans and (b) asymmetric (011) 2θ-ω scans. Arrows indicate the peak positions for the bulk $Ba_{0.5}Sr_{0.5}TiO_3$.

tions. On the other hand, the in-plane lattice parameter a was derived from a combination of the (011) asymmetric and (001) symmetric reflections. Figure 2 shows the lattice parameters a and c as well as the c/a ratio as a function of the film thickness for the BST films. These XRD measurements show that the BST films on STO substrates have a tetragonal distortion with the c lattice constant being larger than that of the bulk material of the same composition. The variation of the lattice parameter c with film thickness is remarkable (from 4.1390 to 4.0552 Å) in the range from 160 nm to 500 nm. Note that the lattice parameter c of the 1000-nm-thick film is almost the same as that for the 500-nm-thick film. On the contrary, the in-plane lattice parameter shows a relatively small change with film thickness. It is suggested that the in-plane lattice parameter a is more confined by the substrate. Similar tetragonal distortion has been reported for BST films grown on MgO substrates, and the observed distortion was correlated with the oxygen pressure during growth presumably due to the generation of oxygen vacancies.[9–12] Oh *et al.*[13] reported the distortion of BST grown on MgO by rf magnetron sputtering and found that the low rf power yielded BST films with less distortion. In deposition experiments by sputtering, either high oxygen pressure or low rf power can lower the growth rate dramatically. A low growth rate can help to relieve strain in growing film at a relatively high growth temperature. Thus, several factors may act in unison to cause such tetragonal distortion. These factors are generally believed to be the lattice mismatch, the difference in the thermal expansion coefficients, and oxygen vacancies. Most likely, the distortion in our films is associated with lattice mismatch, since the thermal mismatch is believed to be negligible and distortion decreases with increasing film thickness due to strain relaxation.

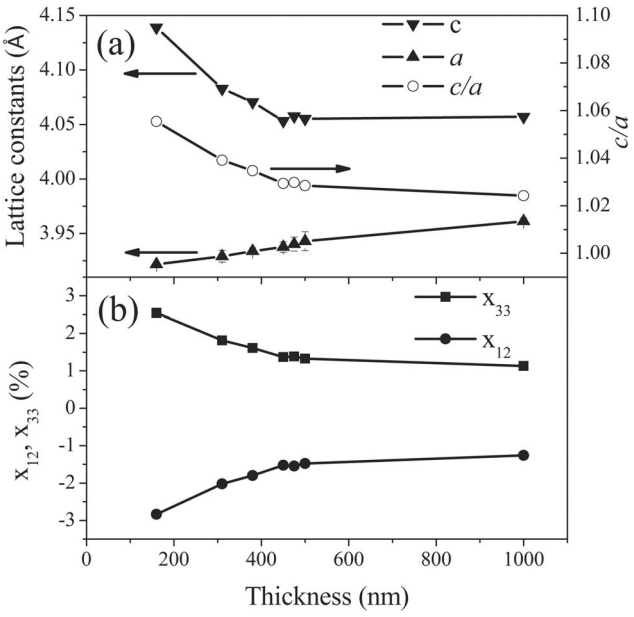

FIG. 2. (a) Lattice parameters (c and a) and c/a ratio, (b) strain (x_{12},x_{33}) of epitaxial BST thin films as a function of the film thickness.

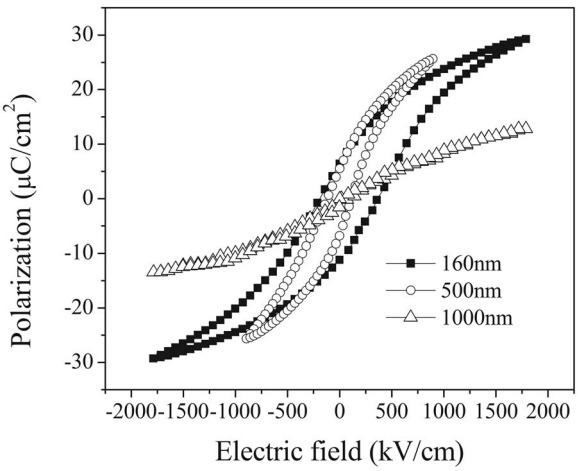

FIG. 3. *P-E* hysteresis loops of BST thin films with various thicknesses measured at 300 K.

In our experiments, the strain state of BST thin films was calculated using $x_{12}=(a-a_0)/a_0$ and $x_{33}=(c-a_0)/a_0$ for in-plane and out-of-plane, respectively. The freestanding cubic lattice constant a_0 of the BST film is estimated from $a_0=[c+2(c_{12}/c_{11})a]/[1+2(c_{12}/c_{11})]$, where c_{11} and c_{12} are the averaged elastic constants of bulk $BaTiO_3$ and $SrTiO_3$.[14] The BST films grown on STO are under large compressive biaxial strain which decreases with increasing thickness of the film as shown in Fig. 2(b). Large strain remains even for the 1000 nm film, where the in-plane and out-of-plane strain values are −1.26% and 1.14%, respectively.

Measurements of the ferroelectric properties and dielectric permittivity for BST films grown on conductive STO: Nb 0.5% substrates (resistivity ~0.05 Ω cm) were undertaken with a *LCR* meter. Use of conductive STO substrate as the bottom electrode provides a simple and accurate way to examine electrical properties and extract their parameters directly. Au/Cr (50 nm/30 nm in thickness) circular top electrodes were patterned on the surface of BST films by using conventional photolithography and lift-off process. The diameter of the top electrode is 200 μm. The ferroelectric properties of the BST films were examined by polarization-electric field (P-E) measurements at $T=300$ K and are shown in Fig. 3. As can be seen, the 160-nm-thick BST film, which has the largest strain among the films measured, displays a pronounced ferroelectric hysteresis loop with a remanent polarization of $P_r=15$ μC/cm^2. The hysteresis loop

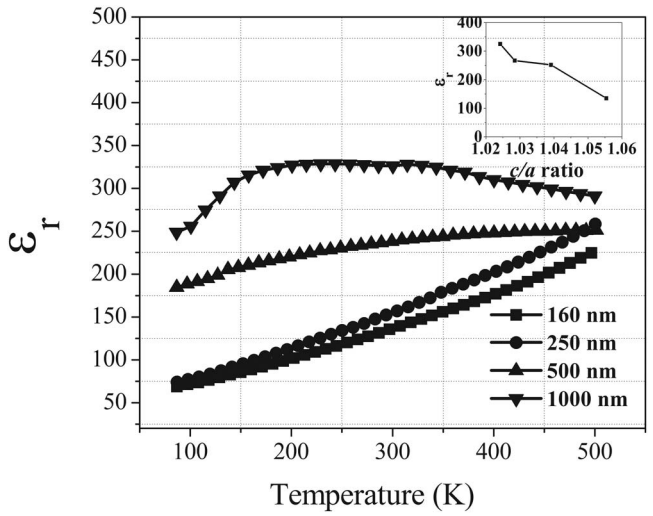

FIG. 4. Out-of-plane dielectric constant in strained BST films as a function of temperature and film thickness. The inset is the dielectric constant as a function of the c/a ratio at 300 K.

for the 1000-nm-thick film at 300 K is barely detected and characterized with a small remanent polarization ($P_r = 1-2\ \mu C/cm^2$). The results of *P-E* measurements indicate that the strain enhances the ferroelectric properties of epitaxial BST thin films.

The relative dielectric constant was measured as a function of temperature for a variety of BST films with thicknesses ranging from 160 to 1 μm. Figure 4 shows the temperature dependence of the out-of-plane dielectric constants ε_r of 160-, 250-, 500-, and 1000-nm-thick BST films measured at 1 MHz. To reiterate, the lattice parameters are very sensitive to the thickness due to strain relaxation of the thin films. The thinner films (160 and 250 nm), with relatively large tetragonal distortion, show temperature dependences of ε_r very dissimilar to those measured for 500- and 1000-nm-thick films. As illustrated in Fig. 4, the values of the dielectric constant in the films with thicknesses of 160 and 250 nm increase steadily with the temperature up to 500 K (the upper limit of our measurement system) indicating no sign of any phase transition. The results imply that T_c of these strained BST films is much higher than that of bulk $Ba_{0.5}Sr_{0.5}TiO_3$ (T_c=250 K). Theory has been proposed to estimate the T_C values of BST thin films under strain.[3] For 160- and 250-nm-thick BST film with large out-of-plane strain x_{33}=2.54% and 2.09%, respectively [see Fig. 2(b)], the predicted T_c in the out-of-plane direction would be around 1300–1500 K, which is far above our measurement temperatures. However, the 500- and 1000-nm-thick films exhibit very weak temperature dependences of the dielectric constant. This weak temperature dependence of the dielectric constant has been attributed to inhomogeneous strain.[15] Considering the large strain remaining in the films, the influence of inhomogeneous strain might be more significant in thick strained films.

The values of dielectric constant in our single crystalline thin films are much lower than that in bulk $Ba_{0.5}Sr_{0.5}TiO_3$ and polycrystalline $Ba_{0.5}Sr_{0.5}TiO_3$ thin films.[16] Small dielectric constant of the BST films agrees well with the theoretical analysis[17] showing that the dielectric constant ε_r decreases under large in-plane compressive strain. As seen from Fig. 2, the thicker the BST thin film is, the smaller the c/a ratio becomes. It indicates that increasing film thickness induces the formation of misfit dislocations which facilitate film relaxation. In addition, the inset in Fig. 4 exhibits the dielectric constant at room temperature as a function of the c/a ratio, which clearly indicates the trend that the dielectric constant ε_r decreases with increasing strain under in-plane compressive strain.

In summary, we have studied strained BST thin films grown on STO substrates by rf magnetron sputtering. The structural properties measured by HRXRD reveal large in-plane compressive strain. The dielectric properties of strained BST films were examined as a function of temperature. The results indicate that strain can significantly change the dielectric properties and lead a large change in the Curie temperature. Large in-plane compressive strain decreases the out-of-plane dielectric constant in BST thin films but enhances their ferroelectric properties.

This work is supported by a grant from the Office of Naval Research with Dr. Ingham Mack being the program manager.

[1] P. Bao, T. J. Jackson, X. Wang, and M. J. Lancaster, J. Phys. D **41**, 063001 (2008).
[2] A. K. Tagantsev, V. O. Sherman, K. F. Astafiev, J. Venkatesh, and N. Setter, J. Electroceram. **11**, 5 (2003).
[3] W. Chang, L. M. B. Alldredge, S. W. Kirchoefer, and J. M. Pond, J. Appl. Phys. **102**, 014105 (2007).
[4] N. A. Pertsev, V. G. Koukhar, R. Waser, and S. Hoffmann, Appl. Phys. Lett. **77**, 2596 (2000).
[5] C. K. Maiti, S. Chattopadhyay, and L. K. Bera, *Strained-Si Heterostructure Field Effect Devices* (CRC, Cleveland, 2007).
[6] J. H. Haeni, P. Irvin, W. Chang, R. Uecker, P. Reiche, Y. L. Li, S. Choudhury, W. Tian, M. E. Hawley, B. Craigo, A. K. Tagantsev, X. Q. Pan, S. K. Streiffer, L. Q. Chen, S. W. Kirchoefer, J. Levy, and D. G. Schlom, Nature (London) **430**, 758 (2004).
[7] K. J. Choi, M. Biegalski, Y. L. Li, A. Sharan, J. Schubert, R. Uecker, P. Reiche, Y. B. Chen, X. Q. Pan, V. Gopalan, L.-Q. Chen, D. G. Schlom, and C. B. Eom, Science **306**, 1005 (2004).
[8] JCPDS-ICDD Card No. 00–039–1395.
[9] W. J. Kim, W. Chang, S. G. Qadri, J. M. Pond, S. W. Kirchoefer, D. B. Chrisey, and J. S. Horwitz, Appl. Phys. Lett. **76**, 1185 (2000).
[10] L. M. B. Alldredge, W. Chang, S. B. Qadri, S. W. Kirchoefer, and J. M. Pond, Appl. Phys. Lett. **90**, 212901 (2007).
[11] W. Chang, J. S. Horwitz, A. C. Carter, J. M. Pond, S. W. Kirchoefer, C. M. Gilmore, and D. B. Chrisey, Appl. Phys. Lett. **74**, 1033 (1999).
[12] L. M. Alldredge, W. Chang, S. W. Kirchoefer, and J. M. Pond, Appl. Phys. Lett. **94**, 052904 (2009).
[13] U. C. Oh, T. S. Kang, K. H. Park, and J. Ho Je, J. Appl. Phys. **86**, 163 (1999).
[14] W. Chang, C. M. Gilmore, W.-J. Kim, J. M. Pond, S. W. Kirchoefer, S. B. Qadri, D. B. Chirsey, and J. S. Horwitz, J. Appl. Phys. **87**, 3044 (2000).
[15] G. Catalan, B. Noheda, J. McAneney, L. J. Sinnamon, and J. M. Gregg, Phys. Rev. B **72**, 020102(R) (2005).
[16] W. Y. Park, K. H. Ahn, and C. S. Hwang, Appl. Phys. Lett. **83**, 4387 (2003).
[17] N. A. Pertsev, A. G. Zembilgotov, and A. K. Tagantsev, Phys. Rev. Lett. **80**, 1988 (1998).